

3D-nanostructured Au electrodes for the event-specific detection of MON810 transgenic maize

M. Fátima Barroso^{a,1}, Maria Freitas^{a,b,1}, M. Beatriz P.P. Oliveira^c,
Noemí de-los-Santos-Álvarez^{b,n}, María Jesús Lobo-Castañón^b, Cristina Delerue-Matos^a

^a REQUIMTE, Instituto Superior de Engenharia do Porto, Instituto Politécnico do Porto, Rua Dr. António Bernardino de Almeida 431, 4200-072 Porto, Portugal

^b Dpto. Química Física y Analítica, Universidad de Oviedo, Av. Julián Clavería 8, 33006 Oviedo, Spain

^c REQUIMTE, Departamento de Ciências Químicas, Faculdade de Farmácia, Universidade do Porto, Rua de Jorge Viterbo Ferreira, 228, Porto 4050-313, Portugal

ABSTRACT

In the present work, the development of a genosensor for the event-specific detection of MON810 transgenic maize is proposed. Taking advantage of nanostructuring, a cost-effective three dimensional electrode was fabricated and a ternary monolayer containing a dithiol, a monothiol and the thiolated capture probe was optimized to minimize the unspecific signals. A sandwich format assay was selected as a way of precluding inefficient hybridization associated with stable secondary target structures. A comparison between the analytical performance of the Au nanostructured electrodes and commercially available screen-printed electrodes highlighted the superior performance of the nanostructured ones. Finally, the genosensor was effectively applied to detect the transgenic sequence in real samples, showing its potential for future quantitative analysis.

Keywords:

GMO, Genosensor, Nanostructured 3D Au electrodes Screen-printed electrodes MON810 maize

1. Introduction

Due to the increase of novel food production and the lack of information and confidence within the society regarding genetically modified organisms (GMO), some governmental regulatory agencies have established compulsory labeling requirements. Indeed, the European Union (EU) legislation demands the labeling of food and feed products containing, consisting of, or produced from GMO in a proportion higher than 0.9% of EU-authorized-GMO material unless its presence is adventitious or technically unavoidable [1]. To guarantee the implementation of these regulations and to ensure consumer's rights to information, it is necessary to monitor and verify the compliance of the labeling by the use of appropriate testing methods to detect GM events in processed food and feed-stuffs [2]. Maize is the second most cultivated GM crop with the largest number of authorized GM events for food and feed [3]. The transgenic MON810 maize, which contains the *cry1Ab* gene inserted to confer insect resistance, was introduced as an authorized transgenic maize event in the EU in 1998, being recently reported as one of the most frequent GM maize events found in foods [4].

Contradictorily, its cultivation is banned in several European countries such as France and Germany [5].

Analytical methods are required for reliable and accurate detection

and quantification of GMO, not only to verify the compliance with legislation, but also to help manufacturers improving their food/feed production in terms of hazard analysis of critical control points (HACCP), risk assessment and good manufacturing practices. DNA-based methods, namely the polymerase chain reaction (PCR), are the techniques of choice for GMO detection. Real-time PCR is the gold standard for quantitative analysis of GMO [6]. The application of DNA-based biosensors in the field of GMO detection and quantification represents a promising technique to explore. Among various types of biosensors, the electrochemical transduction is widely used because it answers to the demands of high sensitivity, specificity, and fast analysis [7]. Moreover, electrochemical biosensors are used in point-of-need devices since they are portable, simple, easy to use, cost effective, and in most cases, disposable.

Basically, an electrochemical sensor for DNA detection is based on the immobilization of an oligonucleotide probe onto the electrode surface and subsequent detection of the complementary strand (the target) by hybridization. These devices have been reported in the literature for the binding of the GMO capture strand onto a surface of carbon or gold electrodes [8–11], or complex nanostructures such as composites of graphene–TiO₂

nanorods [12] and carbon nanotubes [13]. The use of nanostructured materials has been intensely increased since these nanomaterials constitute new platforms for biomolecular sensing that provide improved sensitivity and amenability to miniaturization [14–16].

Gold nanoelectrode ensembles (GNEE) are random arrays of nanoelectrodes typically prepared by electroless deposition of gold within the pores of a microporous polycarbonate (PC) membrane. The physical characteristics of the Au nanostructures can be tuned by selecting the proper diameter and thickness of the membrane [17]. The application of chemical etching onto the GNEE allows the controlled removal of the PC that surrounds the nanoelectrodes, partially exposing the gold nanowires that compose the ensemble, creating a 3 dimensional (3D)-GNEE. This kind of procedure enables increasing the active area of the electrodes, so larger amounts of biorecognition molecules can be bound on the exposed 3D-GNEE [18]. A side-effect of increasing the active area is the increase in the double-layer charging [19] and the unspecific adsorption. To avoid the former, immobilization of DNA through covalent link to the polycarbonate membrane instead of the Au nanowires, which acted only as transducer, was recently proposed [18]. Interestingly, in that work the DNA target was directly labeled with the enzyme, which is not convenient in biosensing, probably to avoid the adsorption of enzyme, or most commonly, enzyme conjugate on bare Au.

The design of the sensing phase through adequate immobilization of probes on the transducer is one of the key steps towards DNA-sensor development to maximize its performance. In this sense, the easiness of self-assembling of commercially available thiolated DNA probes on gold surfaces makes this strategy one of the most widely employed. Classical immobilization through self-assembled monolayer (SAM) formation requires the introduction of a second alkanethiol (binary layer), typically 6 mercapto-1-hexanol (MCH), as a filling spacer to prevent non-specific adsorption of reagents on Au substrate and flat adsorption of DNA strands that hinders the hybridization event [20]. Nevertheless, a modified Au surface with a binary SAM still have small bare regions (pinholes) and surface defects, leading to relatively high background contributions. The introduction of a dithiol as a third component (ternary monolayer) such as dithiothreitol, 1,6-hexanedithiol (HDT), 1,3-propanedithiol and 1,9-nonanedithiol has been recently proposed. Among these dithiols, HDT led to higher hybridization efficiency and antifouling capability [21], as well as extended storage stability [22]. This large effect over the signal to blank ratio is speculated to be related to lying flat arrangement of dithiol on the surface acting as a bridge to passivate those strong adsorption sites [21].

The present work describes, for the first time, the development of a genosensor for the event-specific detection of MON810 maize based on the design of a ternary SAM of HDT/MCH and thiolated DNA capture probe on 3D-GNEE. To improve the selectivity, as well as to avoid strong secondary structures that can hinder the hybridization efficiency, a sandwich hybridization format of the MON810-specific event was developed using a fluorescein isothiocyanate (FITC) labeled signaling DNA probe and enzymatic amplification of the analytical signal. Enzymatic labeling with

monovalent ligands provides an improvement regarding the limits of detection, while simultaneously introducing selectivity to the measurement [23]. A comparison between the nanostructured electrode and a conventional screen-printed electrode (SPGE) was carried out. Finally, the 3D GNEE genosensor was used for the detection of amplified PCR products of certified reference materials containing MON810 maize.

2. Materials and methods

2.1. GM maize materials

Certified reference materials from the Institute for Reference Materials and Measurements (IRMM, Geel, Belgium) were used as standards containing 0% and 5% of MON810 maize event (Fluka, Buchs, Switzerland). A sample of maize flour spiked with 1% of MON810 maize event was obtained from an interlaboratorial study.

2.2. Chemicals and solutions

6-Mercapto-1-hexanol (MCH), 1,6-hexanedithiol (HDT, 96%), dithiothreitol (DTT), enzyme substrate 3,3',5,5'-tetramethylbenzidine (TMB, Neogen K-blue enhanced activity substrate, containing H₂O₂), Trifluoroacetic acid (CF₃COOH), tin(II) chloride, sodium hydrogencarbonate, formaldehyde, methanol, ammonia, ammonium hydroxide, nitric acid (65%), 20 × saline sodium phosphate (200 mM sodium phosphate, 3 M NaCl, 20 mM EDTA) pH

7.4 solution (20 × SSPE) were purchased from Sigma-Aldrich. Silver nitrate and ethanol were acquired from Carlo Erba and Panreac, respectively. Dichloromethane was from Fluka and sodium sulfite, sodium phosphate monohydrate, and sodium dihydrogenphosphate from Riedel-de-Haën. The sodium gold sulfite solution (100 g Au L⁻¹) was obtained from Metakem, casein from Pierce and the conjugated anti-fluorescein-POD Fab fragment was purchased from Roche Diagnostics (Mannheim, Germany).

Track-etch polycarbonate membranes (PC) (pore size of 50 nm, pore density of approximately 9.82 × 10⁵ pores cm⁻², and a thickness of 6–14 mm) were obtained from Whatman (GE Health-care Europe GmbH, Freiburg, Germany). Two different buffers were used: 2 × SSPE, pH 7.4, prepared by 1/10 dilution of 20 × SSPE and binding buffer (BB) (PBS (1 ×) containing 0.5% casein pH 7.2).

The synthetic oligonucleotide sequences and primers were obtained from Sigma-Aldrich (London, UK) and Eurofins MWG Operon (Ebersberg, Germany), respectively, as desalted products. Their sequences are listed in Table 1. All oligonucleotide stock solutions were prepared in Milli-Q water and stored at – 20 °C. Working oligonucleotide solutions were prepared by dilution of an amount of oligo stock solution in 2 × SSPE. The thiol-modified capture probe (CP) was commercially supplied as disulfide. Prior to use, this product was treated with DTT and then purified by elution through a Sephadex G25 column (NAP-10, Amersham Biosciences) with Milli-Q water. After elution, the concentration

Table 1
Oligonucleotide sequences.

DNA strand name	Length	Sequence (5' – 3')
Capture probe (CP)	21	TTA GAG TCC TTC GTC CTT CGA- SH
Signaling probe (FITC-SP)	51	FITC-TCT TCA CAA TAA AGT GAC AGA TAG CTG GGC AAT GGC AAA GGA TGT TAA ACG
Target (T)	72	TCG AAG GAC GAA GGA CTC TAA CGT TTA ACA TCC TTT GCC ATT GCC CAG CTA TCT GTC ACT TTA TTG TGA AGA
Forward primer (Mail-F)	24	TCG AAG GAC GAA GGA CTC TAA CGT
Reverse primer (Mail-R)	24	GCC ACC TTC CTT TTC CAC TAT CTT

of the thiolated oligonucleotide was measured spectrophotometrically at 260 nm and subsequently stored at -20°C until use.

A SuperHot Taq DNA Polymerase with 10 \times buffer containing Tris-HCl (pH 8.8), 160 mM of $(\text{NH}_4)_2\text{SO}_4$, 0.1% of Tween 20 and 25 mM MgCl_2 from Genaxxon Bioscience (Germany) was used for PCR amplification. dNTP were obtained from Bioron (Germany).

All other reagents were of analytical or molecular biology grades. Unless otherwise indicated, double-deionized water (Milli-Q, Millipore Corporation) was used to prepare all aqueous solutions.

The gold plating solution was prepared by dissolving 3.2014 g of Na_2SO_3 , 0.42 g of NaHCO_3 , and 10 mL of HCHO in 180 mL water. The pH of this solution was adjusted to 10 and the volume adjusted to 200 mL with water. Twenty milliliters of this solution were mixed with 0.2 mL of the $\text{Na}_3\text{Au}(\text{SO}_3)_2$ solution and the final pH was again adjusted to 10.

2.3. Instrumentation

Electrochemical measurements were performed by using an autolab PGSTAT12 Potentiostat/Galvanostat with GPES software (version 4.9, EcoChemie, the Netherlands). Chronoamperometry measurements were performed by using two different types of working electrodes: disposable screen-printed electrodes (SPGE) (DRP 220BT, DropSens, Spain) or 3D-GNEE (homemade). SPGE consisted of a 4 mm diameter gold electrode, surrounded by a Au counter electrode and a silver pseudo-reference electrode. When using the 3D-GNEE (2 mm in diameter), a platinum counter electrode and a $\text{Ag}|\text{AgCl}|\text{KCl}_{\text{sat}}$ reference electrode were used. In this case, the 3D-GNEE was immersed in an electrochemical microcell (homemade) with a saline bridge in the bottom to allow the contact with the external conventional electrochemical cell where the microcell, the counter and reference electrodes were immersed. A MJ Mini thermal cycler (BioRad, Hercules, CA, USA) was used for PCR amplification.

2.4. Methodology

2.4.1. Preparation of 3D-GNEE

The 3D-GNEEs were prepared by using polycarbonate membranes (PC) templates (Fig. 1) following the analytical procedure [24] that briefly consisted on: immersion of the PC in a 0.026 M SnCl_2 solution (containing 300 mL of TFA and 50:50 of methanol: water) for 45 min. Then the membrane was washed with methanol for 10 min and activated in ammonia solution containing AgNO_3 solution (0.029 M) for 10 min. To remove the excess of silver, the PC was washed with methanol for 10 min. After that, the PC was placed in a gold plating solution for 24 h (step 1). Then the PC was immersed in water for 10 min and in 25% of HNO_3 for 12 h. The removal of the gold deposited on the PC was carried out by using Q-tips wetted with methanol. Finally, the PC was heated at 150°C for 10 min. To produce a 3D structure an etching procedure

was performed. For that, the gold-filled PC was etched by using Q-tips dipped in a 50:50 $\text{CH}_2\text{Cl}_2/\text{EtOH}$ mixture (step 2). A copper tape was used for electrical contact and the electrochemical area was defined by a teflon mask (step 3). The home-made electrodes have an estimated cost of less than half a euro per unit.

2.4.2. Electrode conditioning

Both SPGE and 3D-GNEE were subjected to several potential cycles between 0 and 1.6 V in 0.1 M H_2SO_4 solution at 100 mV s^{-1} until an ideal redox wave of polycrystalline Au was obtained. The electrochemical surface area of the SPGE and 3D-GNEE was calculated from the charge associated with the gold oxides reduction peak obtained after the cleaning process, assuming that the reduction of the monolayer of gold oxide requires 386 mC cm^{-2} [25].

2.4.3. Preparation of sensing interface

The protocol of the modification is schematized in Fig. 2. A mixture of 0.1 mM of thiol CP and 1 mM of freshly prepared HDT was prepared in 2 \times buffer (from ethanolic concentrated solution) and stood for 10 min. Then, the CP and HDT were immobilized on the Au surface by dropping aliquots of 10 mL of this mixture onto the SPGE or 3D-GNEE to obtain a binary SAM interface (Fig. 2, step 1). Chemisorption was allowed to proceed overnight (16 h), at 4°C , in humidified Petri dishes to protect the solutions from evaporation. Afterwards, the electrode surface was rinsed with Milli-Q water to remove the weakly adsorbed DNA or HDT and dried with nitrogen. The ternary SAM was completed by treatment with the spacer alkanethiol. A 10 mL drop of 1 mM aqueous solution of MCH (prepared in 2 \times buffer) was placed onto the DNA-modified surface for 30 min, washed with Milli-Q water and dried under nitrogen (Fig. 2, step 2).

2.4.4. Sandwich assay format protocol

Before the hybridization reaction, the modified electrode was washed with 2 \times buffer. Both synthetic oligonucleotides and amplified PCR products were analyzed by a sandwich-hybridization format, using fluorescein as a tag in the detection probe, anti-fluorescein-POD as the reporter molecule and a ready-to-use TMB- H_2O_2 solution as a substrate for the electrochemical measurement of the captured POD label. Different concentrations of synthetic DNA target and amplified PCR products were diluted in 2 \times buffer containing 0.5 mM of FITC-signaling probe (FITC-SP). To minimize unintended secondary structure of target, the homogeneous hybridization solutions were thermally denatured at 98°C for 5 min and the strand re-annealing was retarded by cooling the sample in an ice-water bath for 5 min. Then, a heterogeneous hybridization was performed by placing 10 mL of this hybridization solution onto the gold electrodes for 1 h (Fig. 2, step 3).

After hybridization, the modified gold electrodes were rinsed with 2 \times buffer and dried under nitrogen. Then, these electrodes were incubated with 10 mL of 0.5 U mL^{-1} anti-FITC-POD solution

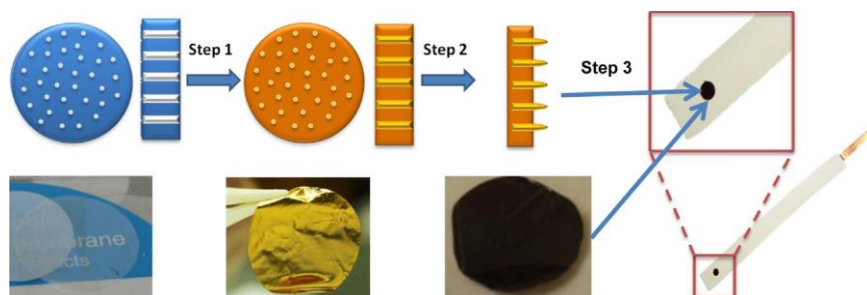


Fig. 1. Schematic representation of the fabrication of 3D-GNEE on polycarbonate membranes.

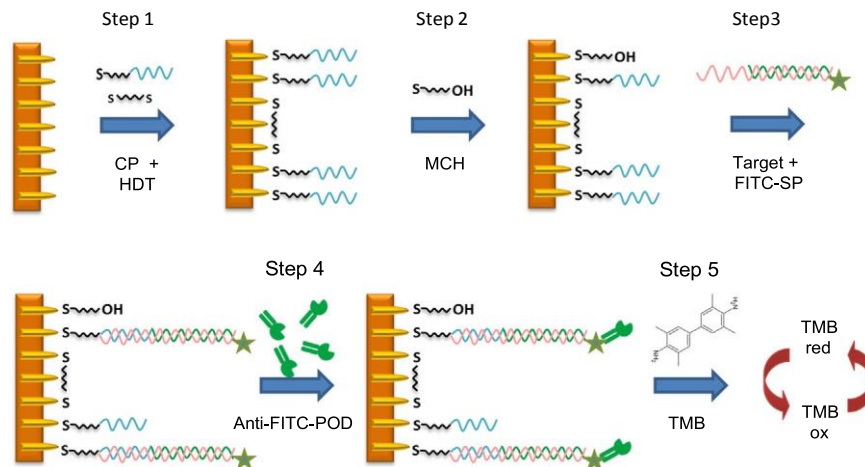


Fig. 2. Schematic representation of the setup for the recognition and electrochemical detection of event-specific DNA sequences from MON810 maize.

in BB for 30 min (Fig. 2, step 4). Subsequently, the electrodes were washed and dried with nitrogen.

To perform the chronoamperometric detection, 40 mL of the TMB- H_2O_2 K-Blue reagent solution was placed sequentially on each of the SPGE, covering the three electrodes area. When 3D-GNEEs were used, 250 mL of the TMB- H_2O_2 K-Blue reagent solution was placed in a microcell and the 3D GNEE was immersed in this solution. After 60 s, the potential was stepped to -200 mV and the current was measured during 60 s (Fig. 2, step 5).

2.4.5. Genomic DNA extraction and PCR amplification

DNA was extracted using the Wizard method as previously described [4]. Yield and purity of extracts were assessed by UV spectrophotometry. The PCR amplifications were carried out in 25 mL of total reaction volume containing 2 mL of DNA extract (200 ng), 1x buffer, 200 mM of each dNTP, 1.0 U of Taq DNA polymerase, 2.0 mM of MgCl_2 and 0.4 mM of each primer Mail-F/ Mail-R (Table 1). The assays were carried out according to the following program: initial denaturation at 95 $^{\circ}\text{C}$ for 5 min; 35 cycles at 95 $^{\circ}\text{C}$ for 30 s, 64 $^{\circ}\text{C}$ for 30 s and 72 $^{\circ}\text{C}$ for 30 s; with a final extension at 72 $^{\circ}\text{C}$ for 5 min.

3. Results and discussion

3.1. Selection of DNA probes for sandwich format assay

The specific detection of MON810 event requires the selection of a specific DNA fragment of the transgenic construct. Since every transformation event result in different location of the inserted DNA within the organism genome, even in the case of the same DNA construction, the specific sequence must be selected at the junction between the recipient genome and the inserted DNA to be event-specific. Initially, the specific 92 bp fragment amplified by primers Mail-F/Mail-R (Table 1) was selected, as described [26], for the event-specific quantitative real-time PCR detection of MON810 event. However, this sequence possesses a strong secondary structure ($\Delta G^{\circ} -12.92$ kcal mol $^{-1}$ calculated using online tools [27] under the assay conditions, which are 25 $^{\circ}\text{C}$ and $[\text{Na}^+] 0.298$ M). From our experience, this high Gibbs energy might result in hindered surface hybridization, so the length of the target was reduced from the 3' end corresponding to the promoter region, which is common for most transgenic constructs and, therefore, unspecific. The resulting 72 nt target containing 37 nt from the maize genome and 35-nt from the promoter has a less stable secondary structure ($\Delta G^{\circ} -7.00$ kcal mol $^{-1}$), more suitable for

genosensing. The specificity of the shorter target was checked using an online tool for DNA sequence alignment [28]. The capture and signaling probes were also designed to minimize secondary structures while forming a perfect duplex structure after hybridization on the electrode surface avoiding fringe regions that are deleterious for the analytical performance [29]. The probe set with the lowest

combination of them was achieved with a 21 nt capture probe ($\Delta G^{\circ} -1.84$ kcal mol $^{-1}$, almost linear) and 51 nt signaling probe ($\Delta G^{\circ} -4.26$ kcal mol $^{-1}$). This ensures a facilitated surface hybridization. The sequences are displayed in Table 1.

3.2. Optimization of the ternary SAM

Fig. 2 shows the schematic representation of the MON810 genosensor assay. The sandwich format increases the selectivity of the assay because two independent hybridization events take place, the homogeneous one between the target and FITC-SP, and the heterogeneous one between the target and FITC-SP hybrid previously formed and the CP on the electrode surface. The enzyme is incorporated through an affinity interaction between the FITC label and an anti-FITC Fab fragment conjugated to a peroxidase. Monovalent labeling is superior to other multivalent systems such as streptavidin-biotin in terms of sensitivity. This is attributed to the potential multiple binding of a single conjugate to several hybridization events on the surface that decreases the amount of enzymatic activity under identical experimental conditions [23,30]. The substrate (3, 3', 5, 5' tetramethylbenzidine: TMB/ H_2O_2) is added for the chronoamperometric monitoring of the MON810 transgenic hybridization. The amount of POD on the electrode is directly proportional to the amount of target effectively hybridized on the surface.

First of all an optimization of the ternary monolayer was carried out on SPGE. Both HDT and the thiolated CP compete for Au adsorption sites, so enough amount of capture probe should be present to obtain reasonable analytical signals along with an adequate amount of dithiol to cover surface irregularities. The effect was evaluated by analyzing the efficiency of the hybridization through recording the cathodic current of the TMB enzymatically oxidized. As starting point, 300 mM of HDT was used in combination with 1 mM of capture probe and subsequent back-filling with 1 mM of MCH [21]. Under these conditions the signal for the target was indistinguishable from the blank (1.47 ± 0.7 for 5 nM vs 1.67 ± 0.9 mA cm $^{-2}$ for the blank). This behavior was assigned to an excessive amount of dithiol that precludes the immobilization of CPs, so lower concentrations of HDT were assayed at a fixed CP concentration and two target levels (5 nM

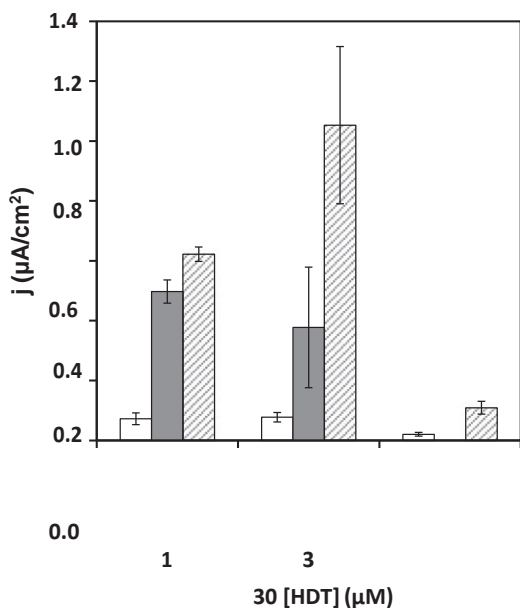


Fig. 3. Variation of the analytical signal expressed as density currents with the composition of the ternary monolayer obtained using 0.5 mM of CP and varying concentrations of HDT overnight. The concentration of MCH was fixed at 1 mM. White bars: blank experiment (no target). Gray bars: 5 nM of synthetic target (72 nt). Striped bars: 50 nM of synthetic target (72-nt). Other conditions as indicated in experimental section.

and 50 nM). From Fig. 3, it is apparent that the hybridization is more effective when low HDT concentrations are used. At 30 mM HDT, the signal for 50 nM was so small in comparison with lower amounts of HDT that the use of such sensing phases was discarded. At 3 mM HDT concentration the current density was higher than at 1 mM but the opposite occurs when testing 5 nM. This indicates that the lower the HDT concentration the higher the CPs available for surface hybridization due to the competition between HDT and CP for the Au binding sites. As a consequence lower amounts of target can be detected with the sensing phases formed from low HDT concentrations. It is worth noting that at low HDT concentrations the saturation is reached at lower target concentrations probably due to electrostatic repulsion of a closely packing DNA monolayer. No significant differences in the blank signals were found even at the relatively low HDT concentrations. As a result, 1 mM HDT was used in further experiments.

Under the optimum HDT concentration, the effect of decreasing the CP was also tested and found favorable. The signal to blank ratio improves from 6.9 when using 0.5 mM CP to 11.3 at 0.1 mM CP. This means that the hybridization was hindered at higher CP concentrations due to the high density of probes on the surface. It is well-known that proper spacing of the ss-DNA probes provides increased accessibility and promotes target capture greatly improving the genosensor performance [16]. Therefore, the concentration of 0.1 mM was selected as the optimum concentration of CP for subsequent studies.

Using the optimized ternary layer, the influence of increasing the synthetic sequence target concentrations on the current was evaluated by using SPGE and 3D-GNEE. In order to compare the results, the electrochemically active area of each type of electrode was calculated from the charge associated to the reduction of the layer of adsorbed oxygen in H_2SO_4 0.1 M (386 mC cm^{-2}) [25]. The analytical signal was then expressed as current density. The average effective area of SPGE and 3D-GNEE was $0.25 \pm 0.04 \text{ (n}\pm 23)$ and $0.10 \pm 0.02 \text{ cm}^2 \text{ (n}\pm 23)$, respectively. This implies a larger average roughness factor for 3D-GNEE (3.4 ± 1.0 versus 2.07 ± 0.3) as anticipated.

Fig. 4 shows the calibration plots in current density using both electrodes in the range between 0.25 and 10 nM MON810. The regression equation for SPGE (black dots) is the following: $j_{net} \text{ (mA cm}^{-2}) = 1.42 \pm 0.03 \text{ [ss-DNA MON810] (nM)} + 7.17 \pm 0.14$,

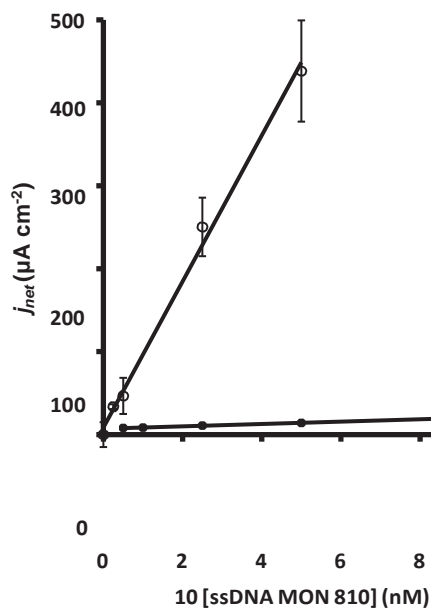


Fig. 4. Variation of the current density with the concentration of synthetic target (72 nt) using SPGE (●) and 3D-GNEE (○) under the optimized conditions up to 10 nM (SPGE) and 5 nM (3D-GNEE).

$r = 0.9995$. The limit of detection (LOD) calculated as three times the standard deviation of the blank divided by the slope of the calibration curve is 0.48 nM. The reproducibility of the analytical response was determined at a target concentration of 2.5 nM presenting a relative standard deviation (RSD) of 5%.

When using 3D-GNEE, the labeling step had to be modified to 45 min. This was attributed to the slower diffusion of the bulky enzymatic conjugate through the finger-like structure of this type of electrode. Under such conditions, a linear relationship between the concentration of the target and the current was also observed between 0.25 and 5 nM (Fig. 4, white dots) with a regression equation $j_{net} \text{ (mA cm}^{-2}) = 9.2 \pm 7.2 \text{ [ss-DNA MON810] (nM)} + 9.2$, $r = 0.997$. From the slope, a 60-fold increase in sensitivity is observed with respect to SPGE. The LOD was 0.25 nM and the reproducibility was 14% for 2.5 nM. This finding is mainly due to the fact that the 3D-GNEE is manually manufactured, leading to somehow dissimilar electrode surfaces as inferred from the standard deviation of the electrochemically active area. This irreproducibility in manufacturing could not be fully compensated by the use of current densities. In spite of this, the 3D-GNEEs were selected for further development. In accordance to the good analytical features and the low-cost fabrication, the 3D-GNEEs were selected for further development. It can be argued that the manufacturing process is long for a disposable electrode, but a great number of electrodes can be prepared simultaneously from a single membrane.

3.3. Application of the 3D-GNEE to detect MON810-specific PCR products

The proposed electrochemical MON810-specific 3D-GNEE genosensor was applied to the detection of amplified PCR products of MON810 transgenic maize event. The genomic DNA of certified reference maize materials containing 5% and 0% of the transgenic event was extracted using the Wizard method. The obtained extracts enabled a DNA yield between 350 and 380 ng mL^{-1} and purity of 1.8, adequate for further PCR amplification. After PCR amplification, the DNA was estimated again spectrophotometrically. Although dNTPs also absorb at 260 nm, this estimation was still valid (as demonstrated below) because of their relatively small concentration after amplification. A calibration plot was constructed with the amplified DNA by diluting different amounts of PCR product in 2x buffer. The PCR amplicon is 20-nt longer than

the synthetic one as previously explained. For that reason, the sandwich assay was designed to keep all extra nucleotides in the DNA end far away from the electrode surface. Hindered hetero- geneous hybridization was previously reported on electrodes when dealing with amplicons with overhangs adjacent to the electrode surface. Consequently, the relative position of the recognition site in the amplicon is of paramount importance to ensure a proper performance. Overhangs as small as 21-nt were found deleterious for the magnitude of the electrochemical signal when using long amplicons (over 200 bp), but not for smaller ones [31]. Recently, an equivalent behavior was also observed with amplicons smaller than 150 bp [32].

Similarly to synthetic oligonucleotides, a denaturation procedure of the amplified DNA by heating at 98 °C for 5 min and cooling in ice bath for 5 min was performed. When using amplicons this step is compulsory due to their double stranded nature. Then 10 mL of denatured specific PCR products were dropped on the modified 3D-GNEE and the hybridization reaction took place at room temperature for 60 min. After the hybridization reaction, the analytical signals were recorded, being presented in Fig. 5 (black dots) for the 5% certified material. As it can be seen, the current is linearly dependent on the total concentration of DNA and perfectly matches the calibration plot with synthetic amplicons (Fig. 5, white dots). The regression equations are: j_{net} (mA cm⁻²) = 3.09 (70.13) [ss-DNA MON810] (pg mL⁻¹) + 9.3 (79.2), r^2 = 0.997 for synthetic oligo (72-nt) and j_{net} (mA cm⁻²) = 2.95 (70.14) [amplicon] (pg mL⁻¹) - 2 (720); r^2 = 0.996 for 92-nt amplicon, respectively. This behavior indicates that the efficiency of the hybridization with a longer strand is similar and the electrochemical signal is not influenced by the presence of a DNA overhang opposite to the electrode surface. In addition, this confirms that the DNA measured spectrophotometrically corresponds to the amplicon. It is worth noting the significant increase in the error bars when approaching saturating target concentration. We speculate that at these concentrations the spatial distribution of the capture probes, which cannot be controlled, decisively influence the hybridization efficiency. In that way, when the capture probes become more evenly distributed the efficiency is higher than when they are closely packed into clusters.

A certified reference material containing no transgenic maize was also evaluated after PCR amplification. The current density for 0% MON810 maize material for a dilution of about 1–1/1900 (less diluted than any 5% sample tested) corresponded to the blank signal within the experimental error, which indicates that the influence of the PCR reagents is negligible on the analytical signal and confirms that it is possible to detect the target fragment without post-PCR purification. To evaluate the applicability of the genosensor, a sample of maize flour with unknown content of MON810 event from an interlaboratory study was also analyzed. After PCR amplification and proper dilution with 2 x buffer

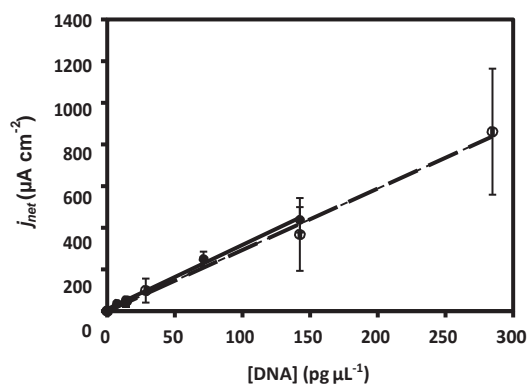


Fig. 5. Variation of the analytical signal with the concentration of DNA (●) from synthetic target (72 nt) and (○) from PCR amplicons (92 bp) using 3D-GNEE.

to obtain a total DNA concentration of 28 pg mL⁻¹, the sample was measured. A blank subtracted j of 47.9 ± 5.0 mA cm⁻² was obtained, which was almost two-times lower than the obtained with the 5% certified sample, suggesting that a lower concentration of transgenic event was present. Considering that the content of MON810 maize event was 1%, according to the interlaboratory study report, the obtained result is in good agreement with the true value. It can be argued that PCR amplifications using more than 30 cycles might fail to correlate with the starting number of DNA copies because of the exhaustion of the exponential growth. However, we previously demonstrated that a non-linear correlation exist beyond the exponential phase when using a hybridization assay for detection. Saturation of the electrode surface that makes the final amplicon concentration independent of the initial DNA template occurs before PCR reaches the plateau. This holds true even after 40 cycles for *Legionella pneumophila* specific sequences with comparable size (95 bp) [33]. Therefore, discrimination between different transgenic percentages is reasonable, even using a high number of PCR cycles and a genosensor as a detection platform. Taking into account that the weight of the haploid genome (C-value) for maize is 2.73 pg [34,35], that maize is hemizygous for MON810 [36] and the starting amount of DNA used in the PCR (200 ng), this approach is able to distinguish between 367 and 1832 initial copies of the transgenic construct.

4. Conclusions

A ternary self-assembled monolayer containing a DNA capture probe for an event-specific sequence of MON810 maize was designed on 3D-GNEE for the detection of the EU approved transgenic maize. The sandwich format with enzymatic amplification was successfully coupled to PCR amplification. Although the resulting amplicon was 20-nt longer than the synthetic oligonucleotide used in the optimization of the method, similar responses were obtained. This is the consequence of a rational design of the sandwich architecture to locate the extra nucleotides at the opposite side of the electrode surface. The analytical performance of the nanostructured Au electrode was superior to that of the commercially available screen-printed electrodes. Large dilutions were needed to carry out the measurement of the amplicons, which indicates that a smaller number of PCR cycles could be enough to detect target construct DNA. Using lower number of cycles, a better discrimination between samples with different GMO contents is expected. Ongoing research is being developed in our labs to establish an empirical correlation between the current measured and the initial copy number with the number of cycles to establish a robust calibration method to reliably quantify maize MON810 at the levels required by the EU for labeling.

Novelty statement

The advantages of using low-cost home-made nanostructured Au electrodes for the construction of genosensors are shown for the first time and applied to the sensitive detection of the most abundant transgenic event authorized in Europe. A simple and rapid method for assessing the presence of unlabeled genetically modified organisms in food is presented.

Acknowledgments

Authors would like to thank Dr. Isabel Mafra and Dr. Joana Costa

for providing the real samples and helpful discussion on PCR amplification. This work has been supported by Fundação para a

Ciência e a Tecnologia (FCT) through Grant no. PEst-C/EQB/LA0006/ 2013, by bilateral project E-38/12 Acções Integradas Luso-Espanholas 2012, Spanish Government through PRI-AIBPT-2011-0769 (International Projects, Acciones integradas luso-españolas) and CTQ2012-31157; and GMOsensor project of International Research StaffExchange Scheme (FP7) PEOPLE-2013-IRSES (Marie Curie actions).

References

- [1] Commission Regulation (EC) No1829, Offi. J. Eur. Union L268 (2003) 1–37.
- [2] I. Mafra, in: M.B.P.P. Oliveira, I. Mafra, Joana S. Amaral (Eds.), *Current Topics on Food Authentication*, Kerala Transworld Research Network, Kerala, India, 2011, pp. 211–236.
- [3] GMO Compass, (<http://www.gmo-compass.org/eng/gmo/db/>), 2014 (accessed 04.02.14).
- [4] T.J.R. Fernandes, J.S. Amaral, M.B.P.P. Oliveira, I. Mafra, *Food Control* 35 (2014) 338–344.
- [5] J. Davison, *Plant Sci.* 178 (2010) 94–98.
- [6] N. Marmiroli, E. Maestri, M. Gulli, A. Malcevski, C. Peano, R. Bordoni, G. De Bellis, *Anal. Bioanal. Chem.* 392 (2008) 369–384.
- [7] M.A. Arugula, Y. Zhang, A.L. Simonian, *Anal. Chem.* 86 (2014) 119–129.
- [8] B. Meric, K. Kerman, G. Marrazza, I. Palchetti, M. Mascini, M. Ozsoz, *Food Control* 15 (2004) 621–626.
- [9] J. Wang, Q.L. Sheng, N. Tian, L.Y. Chen, Z.Q. Xu, J.B. Zheng, *J. Appl. Electrochem.* 39 (2009) 935–945.
- [10] F. Lucarelli, G. Marrazza, M. Mascini, *Biosens. Bioelectron.* 20 (2005) 2001–2009. [11] G. Carpinì, F. Lucarelli, G. Marrazza, M. Mascini, *Biosens. Bioelectron.* 20 (2004) 167–175.
- [12] H.W. Gao, M. Sun, C. Lin, S.B. Wang, *Electroanalysis* 24 (2012) 2283–2290. [13] Q.X. Wang, B. Zhang, X.Q. Lin, W. Weng, *Sens. Actuat. B-Chem.* 156 (2011) 599–605.
- [14] R. Gasparac, B.J. Taft, M.A. Lapierre-Devlin, A.D. Lazareck, J.M. Xu, S.O. Kelley, *J. Am. Chem. Soc.* 126 (2004) 12270–12271.
- [15] L. Soleymani, Z.C. Fang, X.P. Sun, H. Yang, B.J. Taft, E.H. Sargent, S.O. Kelley, *Angew. Chem. Int. Ed.* 48 (2009) 8457–8460.
- [16] X.M. Bin, E.H. Sargent, S.O. Kelley, *Anal. Chem.* 82 (2010) 5928–5931.
- [17] K. Krishnamoorthy, C.G. Zoski, *Anal. Chem.* 77 (2005) 5068–5071.
- [18] M. Silvestrini, L. Fruk, P. Ugo, *Biosens. Bioelectron.* 40 (2013) 265–270.
- [19] M. De Leo, A. Kuhn, P. Ugo, *Electroanalysis* 19 (2007) 227–236.
- [20] A.B. Steel, T.M. Herne, M.J. Tarlov, *Anal. Chem.* 70 (1998) 4670–4677.
- [21] S. Campuzano, F. Kuralay, M.J. Lobo-Castañón, M. Bartosik, K. Vyavahare, E. Palecek, D.A. Haake, J. Wang, *Biosens. Bioelectron.* 26 (2011) 3577–3583. [22] F. Kuralay, S. Campuzano, J. Wang, *Talanta* 99 (2012) 155–160.
- [23] M.J. González-Álvarez, E. Pérez-Ruiz, R. Miranda-Castro, N. de-los-Santos-Álvarez, A.J. Miranda-Ordieres, M.J. Lobo-Castañón, *Electroanalysis* 25 (2013) 147–153.
- [24] A. Pinho, S. Viswanathan, S. Ribeiro, M.B.P.P. Oliveira, C. Delerue-Matos, *J. Appl. Electrochem.* 42 (2012) 131–137.
- [25] A.J. Bard, L.R. Faulkner, *Electrochemical Methods: Fundamentals and Applications*, 2nd ed., John Wiley and Sons Inc, New York, 2001.
- [26] ISO 21570(2005) *Foodstuffs – Methods of analysis for the detection of genetically modified organisms and derived products – Quantitative nucleic acid based methods*, International Standard ISO (2005) 21570, ISO, Geneva.
- [27] M. Zuker, *Nucl. Acids Res.* 31 (2003) 3406–3415.
- [28] (www.ncbi.nlm.nih.gov/BLAST), 2014 (accessed 04.02.14).
- [29] R. Miranda-Castro, P. de-Los-Santos-Alvarez, M.J. Lobo-Castañón, A.J. Miranda-Ordieres, P. Tuñón-Blanco, *Anal. Chem.* 79 (2007) 4050–4055.
- [30] E. Gonzalez-Fernandez, N. de-los-Santos-Alvarez, A.J. Miranda-Ordieres, M.J. Lobo-Castanon, *Sens. Actuat. B-Chem.* 182 (2013) 668–674.
- [31] M.L. Del Giallo, F. Lucarelli, E. Cosulich, E. Pistarino, B. Santamaria, G. Marrazza, M. Mascini, *Anal. Chem.* 77 (2005) 6324–6330.
- [32] B. Martín-Fernández, A.J. Miranda-Ordieres, M.J. Lobo-Castañón, G. Frutos-Cabanillas, N. de-los-Santos-Álvarez, B. López-Ruiz, *Biosens. Bioelectron.* 60 (2014) 244–251.
- [33] R. Miranda-Castro, N. de-los-Santos-Álvarez, M.J. Lobo-Castañón, A.J. Miranda-Ordieres, P. Tuñón-Blanco, *Biosens. Bioelectron.* 24 (2009) 2390–2396.
- [34] Royal Botanic Garden accessible at (<http://data.kew.org/cvalues/>), 2014 (accessed 14.02.14).
- [35] M.D. Bennett, J.B. Smith, *Philos. Trans. Roy. Soc. B* 334 (1991) 309–345. [36] S. Salvi, F. D’Orso, G. Morelli, *J. Agric. Food Chem.* 56 (2008) 4320–4327.